

http://pubs.acs.org/journal/aelccp

Organoammonium-Ion-based Perovskites Can Degrade to Pb⁰ via Amine—Pb(II) Coordination

Junnan Hu, Ross A. Kerner, István Pelczer, Barry P. Rand, and Jeffrey Schwartz*



Cite This: ACS Energy Lett. 2021, 6, 2262-2267



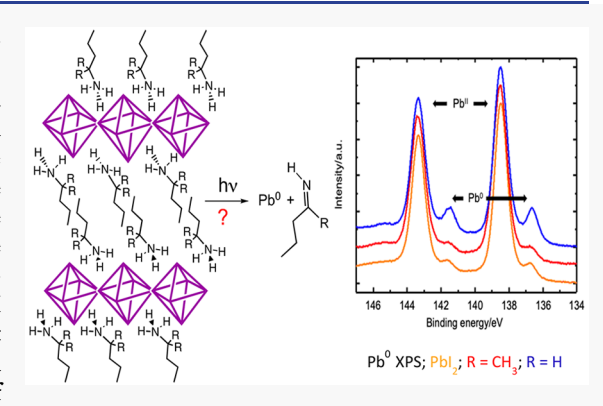
ACCESS

Metrics & More

Article Recommendations

s Supporting Information

ABSTRACT: The degradation of alkylammonium Pb^{II} halide perovskites, in the dark and upon irradiation near room temperature, involves coordinated amine as the dominant reducing agent to yield Pb^{0} near room temperature, as determined by X-ray photoelectron spectroscopy (XPS). The reduction of Pb^{II} first involves amine coordination, supported by ^{207}Pb nuclear magnetic resonance (NMR) analysis. It is shown that a Pb^{II} —amide complex is the immediate precursor of Pb^{II} reduction. Its oxidized counterpart, the imine, is formed and is characterized by NMR and gas chromatography—mass spectrometry. The "redox" process requires a β -C-H bond of the alkylamine. Amine species devoid of this moiety do not similarly reduce Pb^{II} to Pb^{0} . The conversion of an alkylammonium moiety to the Pb^{II} —amide is proposed to occur through a sequence of photoassisted proton-transfer reactions to a lead-coordinated ligand



photoassisted proton-transfer reactions to a lead-coordinated ligand, which is substantiated through XPS-observed Pb^{II} reduction in a family of lead bromide/iodide 2D perovskites.

rganic-based lead halide perovskites have been broadly investigated^{1,2} for photovoltaics,³ lightemitting diodes, 4,5 and lasers and as substrates for fundamental studies of optical and electronic properties.^{7–10} They display defect tolerance, band-gap tunability, and practicable solution processing, but their long-term stability can be problematic and is clearly a prerequisite for practical device utilization. In particular, forming Pb⁰ can be deleterious during fabrication 11 or under operating conditions. 12-15 Sterically small alkylammonium cations (such as methylammonium) are commonly found in crystalline "3D" bulk perovskites; larger ones with broader structural variation are used as spacers in "2D" layered or mixed "2D/3D" species. 8,16-18 While it is commonly assumed that an ammonium lead iodide perovskite can degrade to an amine, HI and PbI₂ that subsequently yields I₂ and Pb⁰, ^{13,19,20} an under-appreciated pathway for formation of Pb⁰ is based instead on the fundamental chemistry of Pb-N bonding: 12,21 PbII and amine nitrogen are "soft" Lewis acids and bases, respectively, and PbII-amine coordination is expected to be strong. Here we show that reduction of PbII to Pb0 can occur by a "redox" reaction in a PbII-coordinated amine, both in the model system, PbI₂, and in a family of 2D perovskites. Indeed, we find that this amine-involved pathway is favored compared with the unimolecular decomposition of PbI₂ to Pb⁰ either in the dark or, more substantially, upon irradiation near room temperature (Figure 1). The key to proving the role of the

amine as the critical reducing agent in our "redox" proposal is the unambiguous identification of its oxidized organic product, the Schiff base. Simply demonstrating the formation of Pb^{012} is insufficient. We further provide evidence to suggest that a Pb^{II} —amide complex is intermediate in the overall sequence for Pb^{II} reduction and that the reduction of Pb^{II} occurs only when a β -C—H moiety is present in the amide ligand. It is especially significant that every step in this sequence involves only simple proton transfer, which apparently is favored under device-relevant stress conditions.

Our proposed pathway for the amine-derived reduction of Pb^{II} is based on a series of simple proton-transfer reactions (Scheme 1) in which it is hypothesized that the coordination of an amine to Lewis-acidic Pb^{II} should result in the acidification of Pb-N-H groups and also any " β -X-H" groups that are present. The final, and key, step in our scheme, the rapid reduction of Pb^{II} to Pb^{0} , is proposed to occur in the coordination sphere of a lead—amide complex. Were this step not fast, direct observation of the amide complex might be possible. Reduction is proposed to occur by the deprotonation

Received: April 5, 2021 Accepted: May 20, 2021 Published: May 25, 2021





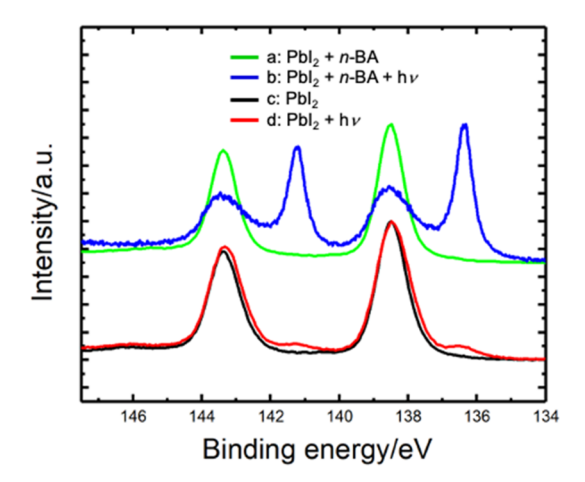


Figure 1. X-ray photoelectron Pb(4f) spectra showing the reduction of Pb^{II} to Pb⁰. (a) Control: PbI₂ before irradiation. (b) PbI₂ following irradiation (1.5 W LED control at 375 nm; intensity ca. 25 mW/cm²) for 18 h. PbI₂ in the presence of n-butylamine (c) before irradiation and (d) upon irradiation. Peaks at ca. 136.5 and 141.5 eV correspond to Pb⁰, and peaks at ca. 138.5 and 143.5 eV correspond to Pb^{II}.

Scheme 1. Reduction of Pb^{II} to Pb⁰ by the Reaction between PbI₂ and Di-iso-propylamine $(1)^a$

^aAmine coordinates to PbI₂. N—H becomes acidified in adduct **2**, as does β -iso-propyl C—H (in blue). The proton transfer from N to iodide give amide complex **3** with the loss of HI. The transfer of β -iso-propyl C—H (in blue) to iodide gives imine complex **4** with the loss of HI and the concomitant reduction of Pb^{II} to Pb⁰, identified by XPS. Imine **5** is identified by NMR and GC-MS. Complex **6** is used for the atomic layer deposition of PbI₂.

of " β -X—H" with the loss of HI. This effectively oxidizes the amine to its dehydrogenated analog, imine 5. We began our studies by examining the chemistry of PbI₂, which is a model for organo-lead perovskites, where it is present as an adduct that is either inadvertently²² or intentionally^{23,24} present in perovskite-based devices. We also examined amines as our first substrate class because they are either added to perovskite formulation mixtures^{25,26} or used in postprocessing. ^{27,28}

To prove that amine—Pb^{II} complexes are readily formed from PbI₂, we probed for coordination by ²⁰⁷Pb NMR in *N*,*N*-dimethylformamide (DMF) solution. Pb/amine ratios were set at *ca*. 1:1. As shown in Figure 2, the reaction with *n*-butylamine (*n*-BA) shows a signal at 1220 ppm that is downfield from that for PbI₂ (955 ppm), as are the signals for the coordination of di-*iso*-propylamine (DiPA; 1090 ppm) and *tert*-butylamine (*t*-BA; 1132 ppm). We attribute the downfield shifts to the replacement of an iodide by a more electronegative nitrogenbased ligand. We relate these differences in ²⁰⁷Pb chemical shifts to the relative steric sizes of the three amine ligands: Cone angles for *n*-alkylamines (106°), *tert*-butyl amine (113°),

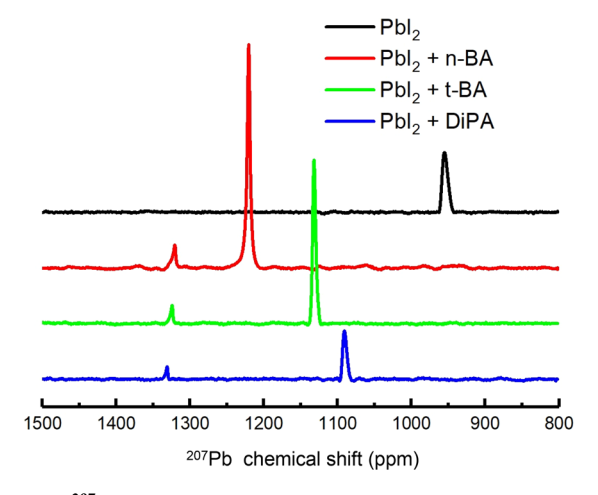


Figure 2. 207 Pb NMR spectra for the reaction between PbI₂ and *n*-butylamine (*n*-BA), di-*iso*-propylamine (DiPA), and *tert*-butylamine (*t*-BA). All spectra were recorded as 0.8 M solutions in DMF, with lead and amine ratios set at *ca.* 1:1.

and di-iso-propylamine (137°) track the relative peak intensities for their complexes in the $^{\rm 207}{\rm Pb}$ NMR spectra from least sterically crowded to most. $^{\rm 29}$ These shifts also correlate with a reduction in nitrogen electronegativity related to the alkyl group donor structure.

Having demonstrated the possibility for lead-amine coordination, we next tested the validity of our overall proposal that rests on the rapid reduction of Pb^{II} to Pb^0 via a lead-amide complex formed between PbI2 and an ex situ prepared amide, lithium di-iso-propylamide (LDA), to give 3 by simple ligation. When a solution of LDA in tetrahydrofuran (THF)/hexanes was added to a suspension of PbI₂ in this solvent mixture at room temperature, the reaction mixture became orange followed by the rapid precipitation of a copious black solid. If the LDA solution was instead added at $-20~^{\circ}\text{C}$ and then allowed to warm, no reaction ensued until ca. -10°C, when a rapid change to orange and then precipitation occurred. After methanol was added to quench any residual LDA, the solid was separated and studied by XPS to confirm its identity as Pb⁰ (Supporting Information, Figure S1). The supernatant was recovered and analyzed by nuclear magnetic resonance (NMR) and gas chromatography-mass spectrometry (GC-MS) (Supporting Information, Figures S2-S5) to show the presence of 5 as the major organic product, which proves our central contention for PbII reduction. It is also important to note here that [bis(trimethylsilyl)amido]lead(II) **6**, which does not have β -C-H bonds, can be prepared from the corresponding lithium amide and isolated as a reagent for use in the atomic layer deposition of lead diiodide.³⁰

Step 2 in Scheme 1 is the conversion of the lead—amine complex 2 to an amide. Given the high reactivity of 3, we can infer with certainty the intermediate formation of 3 by noting its products of decomposition, Pb⁰ and, definitively, 5. In contrast with this latter step that rapidly proceeds even at 0 °C, the treatment of a suspension of PbI₂ with *n*-butylamine at room temperature resulted only in its dissolution, presumably forming the analog of 2. When, however, this solution was placed between two sheets of ITO/glass and irradiated at 375 nm (1.5 W LED light source; illumination intensity *ca.* 25 mW/cm²) for 1 h, Pb⁰ was produced (Supporting Information, Figure S6).

To show further that the reduction to Pb⁰ requires an amine and, in particular, one that contains a β -C-H bond, solid PbI₂ and suspensions of PbI₂ in di-iso-propylamine, tert-butylamine, or dimethylbutylamine or in solution with n-butylamine (PbI₂ is soluble in *n*-butylamine) were irradiated in plain glass vials under the same conditions as previously described (Supporting Information, Figure S7). In no case was Pb⁰ seen in the absence of irradiation, even if the reaction mixtures were heated to 80 °C. Pb⁰ formation on irradiation was observed with di-iso-propylamine and, in particular, with n-butylamine. As expected, 5 was present in the di-iso-propylaminecontaining supernatant (Scheme 1). n-Butylidenebutylamine (7), the adduct of the expected imine (8) with excess nbutylamine, was found in that supernatant (Scheme 2)³¹

Scheme 2. Irradiation of *n*-Butylamine and PbI₂ Gives Imine 8, Which Adds a Second Equivalent of n-Butylamine to Give 7, Identified by GC-MS and NMR by Comparison with **Authentic Material**

$$Pb^{\parallel} \underbrace{\begin{array}{c} 1. \ n\text{-}C_4H_9NH_2 \\ 2. \ hv \end{array}}_{\text{Pb}^0 + \ n\text{-}C_4H_9NH_3^+ \ l^- + \left[\begin{array}{c} N \cdot H \\ N \cdot H \end{array} \right]_{\text{N}} + \left[\begin{array}{c} N \cdot H \\ N \cdot H \end{array} \right]_{\text{N}} + \left[\begin{array}{c} N \cdot H \\ N \cdot H \end{array} \right]_{\text{N}} + \left[\begin{array}{c} N \cdot H \\ N \cdot H \end{array} \right]_{\text{N}} + \left[\begin{array}{c} N \cdot H \\ N \cdot H \end{array} \right]_{\text{N}} + \left[\begin{array}{c} N \cdot H \\ N \cdot H \end{array} \right]_{\text{N}} + \left[\begin{array}{c} N \cdot H \\ N \cdot H \end{array} \right]_{\text{N}} + \left[\begin{array}{c} N \cdot H \\ N \cdot H \end{array} \right]_{\text{N}} + \left[\begin{array}{c} N \cdot H \\ N \cdot H \end{array} \right]_{\text{N}} + \left[\begin{array}{c} N \cdot H \\ N \cdot H \end{array} \right]_{\text{N}} + \left[\begin{array}{c} N \cdot H \\ N \cdot H \end{array} \right]_{\text{N}} + \left[\begin{array}{c} N \cdot H \\ N \cdot H \end{array} \right]_{\text{N}} + \left[\begin{array}{c} N \cdot H \\ N \cdot H \end{array} \right]_{\text{N}} + \left[\begin{array}{c} N \cdot H \\ N \cdot H \end{array} \right]_{\text{N}} + \left[\begin{array}{c} N \cdot H \\ N \cdot H \end{array} \right]_{\text{N}} + \left[\begin{array}{c} N \cdot H \\ N \cdot H \end{array} \right]_{\text{N}} + \left[\begin{array}{c} N \cdot H \\ N \cdot H \end{array} \right]_{\text{N}} + \left[\begin{array}{c} N \cdot H \\ N \cdot H \end{array} \right]_{\text{N}} + \left[\begin{array}{c} N \cdot H \\ N \cdot H \end{array} \right]_{\text{N}} + \left[\begin{array}{c} N \cdot H \\ N \cdot H \end{array} \right]_{\text{N}} + \left[\begin{array}{c} N \cdot H \\ N \cdot H \end{array} \right]_{\text{N}} + \left[\begin{array}{c} N \cdot H \\ N \cdot H \end{array} \right]_{\text{N}} + \left[\begin{array}{c} N \cdot H \\ N \cdot H \end{array} \right]_{\text{N}} + \left[\begin{array}{c} N \cdot H \\ N \cdot H \end{array} \right]_{\text{N}} + \left[\begin{array}{c} N \cdot H \\ N \cdot H \end{array} \right]_{\text{N}} + \left[\begin{array}{c} N \cdot H \\ N \cdot H \end{array} \right]_{\text{N}} + \left[\begin{array}{c} N \cdot H \\ N \cdot H \end{array} \right]_{\text{N}} + \left[\begin{array}{c} N \cdot H \\ N \cdot H \end{array} \right]_{\text{N}} + \left[\begin{array}{c} N \cdot H \\ N \cdot H \end{array} \right]_{\text{N}} + \left[\begin{array}{c} N \cdot H \\ N \cdot H \end{array} \right]_{\text{N}} + \left[\begin{array}{c} N \cdot H \\ N \cdot H \end{array} \right]_{\text{N}} + \left[\begin{array}{c} N \cdot H \\ N \cdot H \end{array} \right]_{\text{N}} + \left[\begin{array}{c} N \cdot H \\ N \cdot H \end{array} \right]_{\text{N}} + \left[\begin{array}{c} N \cdot H \\ N \cdot H \end{array} \right]_{\text{N}} + \left[\begin{array}{c} N \cdot H \\ N \cdot H \end{array} \right]_{\text{N}} + \left[\begin{array}{c} N \cdot H \\ N \cdot H \end{array} \right]_{\text{N}} + \left[\begin{array}{c} N \cdot H \\ N \cdot H \end{array} \right]_{\text{N}} + \left[\begin{array}{c} N \cdot H \\ N \cdot H \end{array} \right]_{\text{N}} + \left[\begin{array}{c} N \cdot H \\ N \cdot H \end{array} \right]_{\text{N}} + \left[\begin{array}{c} N \cdot H \\ N \cdot H \end{array} \right]_{\text{N}} + \left[\begin{array}{c} N \cdot H \\ N \cdot H \end{array} \right]_{\text{N}} + \left[\begin{array}{c} N \cdot H \\ N \cdot H \end{array} \right]_{\text{N}} + \left[\begin{array}{c} N \cdot H \\ N \cdot H \end{array} \right]_{\text{N}} + \left[\begin{array}{c} N \cdot H \\ N \cdot H \end{array} \right]_{\text{N}} + \left[\begin{array}{c} N \cdot H \\ N \cdot H \end{array} \right]_{\text{N}} + \left[\begin{array}{c} N \cdot H \\ N \cdot H \end{array} \right]_{\text{N}} + \left[\begin{array}{c} N \cdot H \\ N \cdot H \end{array} \right]_{\text{N}} + \left[\begin{array}{c} N \cdot H \\ N \cdot H \end{array} \right]_{\text{N}} + \left[\begin{array}{c} N \cdot H \\ N \cdot H \end{array} \right]_{\text{N}} + \left[\begin{array}{c} N \cdot H \\ N \cdot H \end{array} \right]_{\text{N}} + \left[\begin{array}{c} N \cdot H \\ N \cdot H \end{array} \right]_{\text{N}} + \left[\begin{array}{c} N \cdot H \\ N \cdot H \end{array} \right]_{\text{N}} + \left[\begin{array}{c} N \cdot H \\ N \cdot H \end{array} \right]_{\text{N}} + \left[\begin{array}{c} N \cdot H \\ N \cdot H \right]_{\text{N}} + \left[\begin{array}{c} N \cdot H \\$$

(Supporting Information, Figures S8 and S9). Significantly, no Pb⁰ was observed in the similarly treated PbI₂ suspension in *tert*-butylamine or in dimethylbutylamine, which have no β -C-H bonds. Here unidentified colorless solids resulted. These results further emphasize the role of β -C-H bonds in the "redox" formation of Pb⁰ (Step 3 of Scheme 1). They also show that Step 2 of Scheme 1 is photoassisted.

Translating the role of amines in the reduction of Pb^{II} to establish the role of ammonium halide adducts is paramount with regard to understanding the reactivity of the materials that are based on layered 2D or 2D/3D perovskites. 1,8,18 These layers are separated by alkylammonium ions, including linear 18,32,33 amd aminoalkyl-aromatic, 18,34–39 -cycloalkyl, and -heterocyclic ions. 18,35 These can be related to our model through a series of proton-transfer reactions (Scheme

Scheme 3. *n*-Butylammonium ion (*n*-BA⁺) is Hydrogen-Bonded to the Perovskite (9) and Is Converted to the Corresponding Amine Adduct (10) Simply by (N-H)⁺ Group Deprotonation by Iodide, Which Also Yields HIa

^aA second similar loss of HI opens a site on Pb^{II} for amine coordination (3'). Complex 11, which has no β -C-H bonds, cannot act as a similar reducing agent.

We chose to examine n-butylammonium (n-BA⁺) 2D perovskites $(n = 1)^{16}$ as representative materials, several of which we characterized by X-ray diffraction (XRD) (Supporting Information, Figure S10). All studies were done on spincast thin films. We used four halide stoichiometries^{38–40} to further probe the effect of the ammonium salt and the key proposed role of proton transfer from the salt to the "PbX₄" unit. We find by XPS analysis (Supporting Information, Figure S11) that for two of these cases, Pb⁰ is formed in the dark, but more Pb⁰ is produced on irradiation for all four. It is significant that the formation of Pb⁰, both in the dark and upon irradiation, is greatest for the iodide-based perovskite n-BA₂PbI₄. It decreases with the increasing incorporation of Br in place of iodide and is lowest for n-BA₂PbBr₄ (Figure 3). We believe these data are consistent with the first steps shown in the Scheme 3: The iodide species should be more basic than the bromide-substituted species given the relative electro-

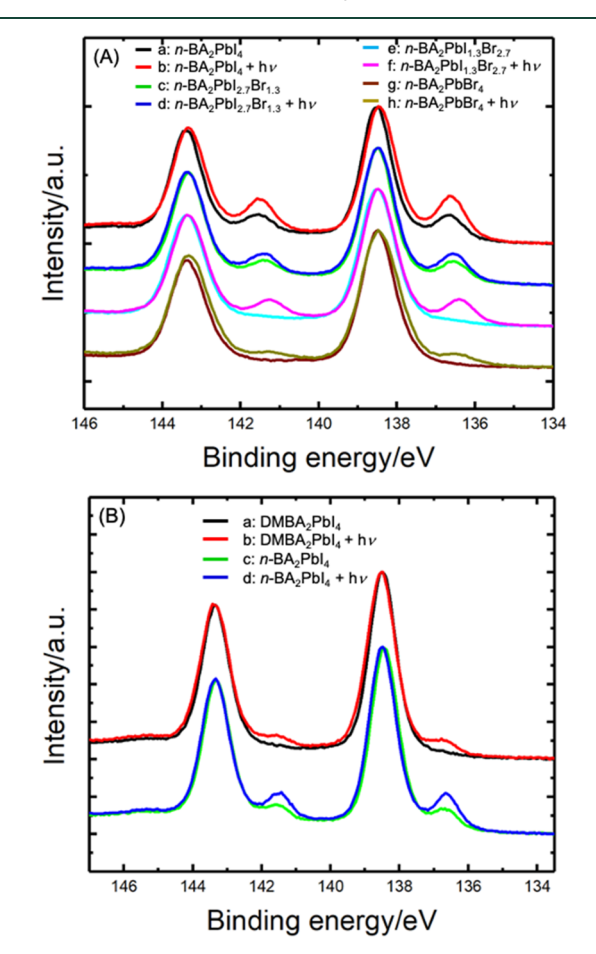


Figure 3. (A) Pb(4f) XPS showing the effect of *n*-butylammoniunm (n-BA+) on the reduction of PbII to Pb0, both in the dark (18 h) and following irradiation (1.5 W LED at 375 nm; intensity ca. 25 mW/cm²), for 18 h for a series of 2D perovskites and a PbI₂ control. (a) n-BA₂PbI₄ in the dark, (b) irradiated n-BA₂PbI₄, (c) mixed halide species n-BA2PbI2.7Br1.3 in the dark, (d) irradiated n-BA₂PbI_{2.7}Br_{1.3}, (e) n-BA₂PbI_{1.3}Br_{2.7} in the dark, (f) irradiated n-BA₂PbI_{1,3}Br_{2,7}, (g) n-BA₂PbBr₄ in the dark, and (h) irradiated n-BA₂PbBr₄. (B) XP Pb(4f) spectra contrasting the effects of nbutylamine (BA) versus dimethylbutylamine (DMBA) on the reduction of PbII to Pb0, both in the dark (18 h) and following irradiation (1.5 W LED at 375 nm), for 18 h. (a) DMBA₂PbI₄ in the dark, (b) irradiated DMBA2PbI4, (c) n-BA2PbI4 in the dark, and (d) irradiated n-BA2PbI4.

negativities of the two halides. Note, in particular, the relatively small amount of Pb^0 formed with the β -C-H-devoid ammonium $DMBA_2PbI_4$ (11) compared with the linear ammonium n-BA $_2PbI_4$, which is attributed to the irradiative reduction of PbI_2 itself (*cf.* Figure 1).

We have shown that the commonly invoked pathway for the formation of Pb⁰ upon irradiation of a simple hybrid organicinorganic lead halide perovskite, decomposition to amine plus PbI₂, and then photolysis to Pb⁰ and I₂ is inefficient compared with a direct amine-based pathway. We further showed that Pb^{II} is reduced to Pb⁰ by a process of β -hydrogen elimination in a key Pb-amide complex intermediate. This process is analogous to the base-assisted dehydrohalogenation of an alkyl halide. It is a reductive process that is well known in the organometallic chemistry of transition metals in that when PbII acts as a "leaving group" following β -hydrogen loss from the amide complex, it retains the pair of electrons that had been in the Pb-N bond. The organic product, the imine, is the formal oxidized product of lead reduction. It is important to note that starting from an organoammonium-ion-incorporated perovskite, several steps involving the likely reversible loss of HI are required to yield first the coordinated amine and then the key lead-amide intermediate.

We demonstrated that the decomposition of a bona fide lead—amide complex to Pb^0 is fast. If all reversible steps leading to the loss of HI were favorable, then we would expect the rapid reduction of our 2D perovskite-based Pb^{II} in the dark, which is contrary to observation. Thus we propose that the role of irradiation is to "pump" proton-transfer reactions⁴¹ to favor HI loss in each step in Scheme 1. In support of this proposed role of proton transfer, we showed that replacing iodide with bromide imparted photochemical stability to our 2D material. Finally, and of perhaps greater significance, we found that an alkylammonium iodide can be used to make a crystalline 2D material that is even more stable to photochemical degradation because the amine is devoid of β -C—H bonds.

To predict classes of ammonium species whose chemistry might preclude the ultimate formation of Pb⁰ requires an analysis of the nature of the organic product that would be formed by putative β -C-H bond elimination. Indeed, there are classes of ammonium species that do contain β -C-H bonds, yet they do not react following deprotonation by β -C-H elimination to give Pb⁰, for example, the common perovskite "A-site" organic cation formamidinium (FA, 12a), where autodecomposition of the formamidine parent (12b) to HCN and ammonia is rapid⁴² (see also Supporting Information, Figure S12), or methylammonium (MA, 13a), where β -C-H elimination from methylamine (13b) would be slow because of the highly reactive, unsubstituted parent imine product, methylenimine, 43 13c (see also Supporting Information, Figure S13) (Scheme 4). Irradiation of inorganic cesium perovskite, formed from CsI and PbI₂, gave no Pb⁰, showing the key role of an amine as a reducing agent (Supporting Information, Figure S14). Finally, there are families of sterically constrained, tertiary amines, such as 1-azabicyclo [2.2.2] octane (14a), where β -elimination would yield a highly strained "bridgehead" olefin (14b).44 Through the consideration of these facets of structure, the design and implementation of amine-based groups that do not promote the deleterious formation of Pb⁰ can be envisaged.

Scheme 4. β -C-H Elimination to Give Pb⁰ is Unfavorable for 12b, Where Decomposition to HCN and NH₃ is Rapid, 13b, where β -C-H Elimination Would Be Very Slow Because of the High Energy of the Parent Imine 13c, and 14a, Where the "Bridgehead" Olefin 14b is Highly Strained

ASSOCIATED CONTENT

Supporting Information

The Supporting Information is available free of charge at https://pubs.acs.org/doi/10.1021/acsenergylett.1c00714.

Complete experimental procedures, five XPS figures, one XRD figure, four sets of NMR spectra, two sets of GC-MS data, and two sets of photographs of lead halide reduction (PDF)

AUTHOR INFORMATION

Corresponding Author

Jeffrey Schwartz — Department of Chemistry, Princeton University, Princeton, New Jersey 08544, United States; orcid.org/0000-0001-9873-4499; Email: jschwart@princeton.edu

Authors

Junnan Hu — Department of Electrical Engineering, Princeton University, Princeton, New Jersey 08544, United States;
orcid.org/0000-0001-7418-8964

Ross A. Kerner — Department of Electrical Engineering, Princeton University, Princeton, New Jersey 08544, United States; © orcid.org/0000-0002-3692-6820

István Pelczer − Department of Chemistry, Princeton University, Princeton, New Jersey 08544, United States; orcid.org/0000-0002-7806-6101

Barry P. Rand – Department of Electrical Engineering and Andlinger Center for Energy and the Environment, Princeton University, Princeton, New Jersey 08544, United States; orcid.org/0000-0003-4409-8751

Complete contact information is available at: https://pubs.acs.org/10.1021/acsenergylett.1c00714

Notes

The authors declare no competing financial interest.

ACKNOWLEDGMENTS

This work was supported by the United States Department of Energy's Office of Energy Efficiency and Renewable Energy (EERE) under their Solar Energy Technology Office (SETO) Award Number DE-EE0008560. We acknowledge the use of Princeton's Imaging and Analysis Center, which is partially

supported through the Princeton Center for Complex Materials (PCCM), a National Science Foundation (NSF)-MRSEC program (DMR-2011750). We also thank Dr. John Eng for help with GC-MS analyses.

REFERENCES

- (1) Saparov, B.; Mitzi, D. B. Organic–Inorganic Perovskites: Structural Versatility for Functional Materials Design. *Chem. Rev.* **2016**, *116*, 4558–4596.
- (2) Zhu, X. The Perovskite Fever and Beyond. Acc. Chem. Res. 2016, 49, 355-356.
- (3) Nayak, P.; Mahesh, S.; Snaith, H. J.; Cahen, D. Photovoltaic solar cell technologies: analysing the state of the art. *Nat. Rev. Mater.* **2019**, *4*, 269–285.
- (4) Van Le, Q.; Jang, H. W.; Kim, S. Y. Recent Advances toward High-Efficiency Halide Perovskite Light-Emitting Diodes: Review and Perspective. *Small Methods* **2018**, *2*, 1700419.
- (5) Sutherland, B. R.; Sargent, E. H. Perovskite photonic sources. *Nat. Photonics* **2016**, *10*, 295–302.
- (6) Zhang, Q.; Shang, Q.; Su, R.; Do, T. H. D.; Xiong, Q. Halide Perovskite Semiconductor Lasers: Materials, Cavity Design, and Low Threshold. *Nano Lett.* **2021**, *21*, 1903–1914.
- (7) Lu, H.; Xiao, C.; Song, R.; Li, T.; Maughan, A. E.; Levin, A.; Brunecky, R.; Berry, J. J.; Mitzi, D. B.; Blum, V.; Beard, M. C. Highly Distorted Chiral Two-Dimensional Tin Iodide Perovskites for Spin Polarized Charge Transport. *J. Am. Chem. Soc.* **2020**, *142*, 13030–13040.
- (8) Zhang, F.; Lu, H.; Tong, J.; Berry, J. J.; Beard, M. C.; Zhu, K. Advances in two-dimensional organic—inorganic hybrid perovskites. *Energy Environ. Sci.* **2020**, *13*, 1154–1186.
- (9) Jana, M. K.; Song, R.; Liu, H.; Khanal, D. R.; Janke, S. M.; Zhao, R.; Liu, C.; Valy Vardeny, Z.; Blum, V.; Mitzi, D. B. Organic-to-inorganic structural chirality transfer in a 2D hybrid perovskite and impact on Rashba-Dresselhaus spin-orbit coupling. *Nat. Commun.* 2020, 11, 4699.
- (10) Liu, X.; Chanana, A.; Huynh, U.; Xue, F.; Haney, P.; Blair, S.; Jiang, X.; Vardeny, Z. V. Circular photogalvanic spectroscopy of Rashba splitting in 2D hybrid organic—inorganic perovskite multiple quantum wells. *Nat. Commun.* **2020**, *11*, 323.
- (11) Sadoughi, G.; Starr, D. E.; Handick, E.; Stranks, S. D.; Gorgoi, M.; Wilks, R. G.; Bär, M.; Snaith, H. J. Observation and Mediation of the Presence of Metallic Lead in Organic–Inorganic Perovskite Films. ACS Appl. Mater. Interfaces 2015, 7, 13440–13444.
- (12) Kerner, R. A.; Schloemer, T. H.; Schulz, P.; Berry, J. J.; Schwartz, J.; Sellinger, A.; Rand, B. P. Amine additive reactions induced by the soft Lewis acidity of Pb²⁺ in halide perovskites. Part I: evidence for Pb—alkylamide formation. *J. Mater. Chem. C* **2019**, 7, 5251—5259.
- (13) Steirer, K. X.; Schulz, P.; Teeter, G.; Stevanovic, V.; Yang, M.; Zhu, K.; Berry, J. J. Defect Tolerance in Methylammonium Lead Triiodide Perovskite. *ACS Energy Lett.* **2016**, *1*, 360–366.
- (14) Zhao, L.; Tian, H.; Silver, S. H.; Kahn, A.; Ren, T.-L.; Rand, B. P. Ultrasensitive Heterojunctions of Graphene and 2D Perovskites Reveal Spontaneous Iodide Loss. *Joule* **2018**, *2*, 2133–2144.
- (15) Hofstetter, Y. J.; Garcia-Benito, I.; Paulus, F.; Orlandi, S.; Grancini, G.; Vaynzof, Y. Vacuum-Induced Degradation of 2D Perovskites. *Front. Chem.* **2020**, *8*, 1–10.
- (16) Stoumpos, C. C.; Cao, D. H.; Clark, D. J.; Young, J.; Rondinelli, J. M.; Jang, J. I.; Hupp, J. T.; Kanatzidis, M. G. Ruddlesden—Popper Hybrid Lead Iodide Perovskite 2D Homologous Semiconductors. *Chem. Mater.* **2016**, *28*, 2852–2867.
- (17) Liang, C.; Zhao, D.; Li, Y.; Li, X.; Peng, S.; Shao, G.; Xing, G. Ruddlesden—Popper Perovskite for Stable Solar Cells. *Energy Environ. Mater.* **2018**, *1*, 221–231.
- (18) Mao, L.; Stoumpos, C. C.; Kanatzidis, M. G. Two-Dimensional Hybrid Halide Perovskites: Principles and Promises. *J. Am. Chem. Soc.* **2019**, *141*, 1171–1190.

- (19) Juarez-Perez, E. J.; Ono, L. K.; Maeda, M.; Jiang, Y.; Hawash, Z.; Qi, Y. Photodecomposition and thermal decomposition in methylammonium halide lead perovskites and inferred design principles to increase photovoltaic device stability. *J. Mater. Chem. A* **2018**, *6*, 9604–9612.
- (20) Roose, B.; Dey, K.; Chiang, Y.-H.; Friend, R. H.; Stranks, S. D. Critical Assessment of the Use of Excess Lead Iodide in Lead Halide Perovskite Solar Cells. *J. Phys. Chem. Lett.* **2020**, *11*, 6505–6512.
- (21) Kerner, R. A.; Schloemer, T. H.; Schulz, P.; Berry, J. J.; Schwartz, J.; Sellinger, A.; Rand, B. P. Amine additive reactions induced by the soft Lewis acidity of Pb²⁺ in halide perovskites. Part II: impacts of amido Pb impurities in methylammonium lead triiodide thin films. *J. Mater. Chem. C* **2019**, *7*, 5244–5250.
- (22) Xu, H.; Wu, Y.; Cui, J.; Ni, C.; Xu, F.; Cai, J.; Hong, F.; Fang, Z.; Wang, W.; Zhu, J.; Wang, L.; Xu, R.; Xu, F. Formation and evolution of the unexpected PbI₂ phase at the interface during the growth of evaporated perovskite films. *Phys. Chem. Chem. Phys.* **2016**, 18, 18607–18613.
- (23) Park, B.-w.; Kedem, N.; Kulbak, M.; Lee, D. Y.; Yang, W. S.; Jeon, N. J.; Seo, J.; Kim, G.; Kim, K. J.; Shin, T. J.; Hodes, G.; Cahen, D.; Seok, S. I. Understanding how excess lead iodide precursor improves halide perovskite solar cell performance. *Nat. Commun.* **2018**, *9*, 3301.
- (24) Jacobsson, T. J.; Correa-Baena, J.-P.; Halvani Anaraki, E.; Philippe, B.; Stranks, S. D.; Bouduban, M. E. F.; Tress, W.; Schenk, K.; Teuscher, J.; Moser, J.-E.; Rensmo, H.; Hagfeldt, A. Unreacted PbI₂ as a Double-Edged Sword for Enhancing the Performance of Perovskite Solar Cells. *J. Am. Chem. Soc.* **2016**, *138*, 10331–10343.
- (25) Liu, Z.; Hu, J.; Jiao, H.; Li, L.; Zheng, G.; Chen, Y.; Huang, Y.; Zhang, Q.; Shen, C.; Chen, Q.; Zhou, H. Chemical Reduction of Intrinsic Defects in Thicker Heterojunction Planar Perovskite Solar Cells. *Adv. Mater.* **2017**, 29, 1606774.
- (26) Noel, N. K.; Habisreutinger, S. N.; Wenger, B.; Klug, M. T.; Hörantner, M. T.; Johnston, M. B.; Nicholas, R. J.; Moore, D. T.; Snaith, H. J. A low viscosity, low boiling point, clean solventsystem for the rapid crystallisation of highly specular perovskite films. *Energy Environ. Sci.* **2017**, *10*, 145–152.
- (27) Lee, S.; Park, J. H.; Lee, B. R.; Jung, E. D.; Yu, J. C.; Di Nuzzo, D. D.; Friend, R. H.; Song, M. H. Amine-Based Passivating Materials for Enhanced Optical Properties and Performance of Organic—Inorganic Perovskites in Light-Emitting Diodes. *J. Phys. Chem. Lett.* **2017**, *8*, 1784–1792L.
- (28) Lin, Y.; Bai, Y.; Fang, Y.; Chen, Z.; Yang, S.; Zheng, X.; Tang, S.; Liu, Y.; Zhao, J.; Huang, J. Enhanced Thermal Stability in Perovskite Solar Cells by Assembling 2D/3D Stacking Structures. *J. Phys. Chem. Lett.* **2018**, *9*, 654–658.
- (29) Seligson, A. L.; Trogler, W. C. Cone Angles for Amine Ligands. X-ray Crystal Structures and Equilibrium Measurements for Ammonia, Ethylamine, Diethylamine, and Triethylamine Complexes with the (Bis(dimethylphosphino)ethane)methylpalladium(II) Cation. J. Am. Chem. Soc. 1991, 113, 2520–2527.
- (30) Popov, G.; Mattinen, M.; Hatanpää, T.; Vehkamäki, M.; Kemell, M.; Mizohata, K.; Räisänen, J.; Ritala, M.; Leskelä, M. Atomic Layer Deposition of PbI₂ Thin Films. *Chem. Mater.* **2019**, *31*, 1101–1109.
- (31) Layer, R. W. The Chemistry of Imines. Chem. Rev. 1963, 63, 489-510.
- (32) Wang, Z.; Lin, Q.; Chmiel, F. P.; Sakai, N.; Herz, L. M.; Snaith, H. J. E-fficient ambient-air-stable solar cells with 2D–3D heterostructured butylammonium-caesium-formamidinium lead halide perovskites. *Nat. Energy* **2017**, *2*, 1–10.
- (33) Xiao, Z.; Kerner, R. A.; Zhao, L.; Tran, N. L.; Lee, K. M.; Koh, T.-W.; Scholes, G. D.; Rand, B. P. Efficient perovskite light-emitting diodes featuring nanometre-sized crystallites. *Nat. Photonics* **2017**, *11*, 108–115.
- (34) Cho, K. T.; Grancini, G.; Lee, Y.; Oveisi, E.; Ryu, J.; Almora, O.; Tschumi, M.; Schouwink, P. A.; Seo, G.; Heo, S.; Park, J.; Jang, J.; Paek, S.; Garcia-Belmonte, G.; Nazeeruddin, M. K. Selective growth

- of layered perovskites for stable and efficient photovoltaics. *Energy Environ. Sci.* **2018**, *11*, 952–959.
- (35) Liu, Y.; Akin, S.; Pan, L.; Uchida, R.; Arora, N.; Milic, J. V.; Hinderhofer, A.; Schreiber, F.; Uhl, A. R.; Zakeeruddin, S. M.; Hagfeldt, A.; Dar, M. I.; Gratzel, M. Ultrahydrophobic 3D/2D fluoroarene bilayer-based water-resistant perovskite solar cells with efficiencies exceeding 22%. Sci. Adv. 2019, 5, eaaw2543.
- (36) Ng, Y. F.; Febriansyah, B.; Jamaludin, N. F.; Giovanni, D.; Yantara, N.; Chin, X. Y.; Tay, Y. B.; Sum, T. C.; Mhaisalkar, S.; Mathews, N. Design of 2D Templating Molecules for Mixed-Dimensional Perovskite Light-Emitting Diodes. *Chem. Mater.* **2020**, 32, 8097–8105.
- (37) Fu, W.; Liu, H.; Shi, X.; Zuo, L.; Li, X.; Jen, A. K.-Y. Tailoring the Functionality of Organic Spacer Cations for Efficient and Stable Quasi-2D Perovskite Solar Cells. *Adv. Funct. Mater.* **2019**, 29, 1900221.
- (38) Febriansyah, B.; Giovanni, D.; Ramesh, S.; Koh, T. M.; Li, Y.; Sum, T. C.; Mathews, N.; England, J. Inducing formation of a corrugated, white-lightemitting 2D lead-bromide perovskite via subtle changes in templating cation. *J. Mater. Chem. C* **2020**, *8*, 889–893.
- (39) Cohen, B.-E.; Wierzbowska, M.; Etgar, L. High efficiency quasi 2D lead bromide perovskite solar cells using various barrier molecules. *Sustain. Energy Fuels* **2017**, *1*, 1935–1943.
- (40) La-Placa, M.-G.; Guo, D.; Gil-Escrig, L.; Palazon, F.; Sessolo, M.; Bolink, H. J. Dual-source vacuum deposition of pure and mixed halide 2D perovskites: thin film characterization and processing guidelines. *J. Mater. Chem. C* **2020**, *8*, 1902–1908.
- (41) Peng, C.-Y.; Shen, J.-Y.; Chen, Y.-T.; Wu, P.-J.; Hung, W.-Y.; Hu, W.-P.; Chou, P.-T. Optically Triggered Stepwise Double-Proton Transfer in an Intramolecular Proton Relay: A Case Study of 1,8-Dihydroxy-2-naphthaldehyde. J. Am. Chem. Soc. 2015, 137, 14349—14357.
- (42) Juarez-Perez, E. J.; Ono, L. K.; Qi, Y. Thermal degradation of formamidinium based lead halide perovskites into sym-triazine and hydrogen cyanide observed by coupled thermogravimetry-mass spectrometry analysis. *J. Mater. Chem. A* **2019**, *7*, 16912–16919.
- (43) Peel, J. B.; Willett, G. D. Methylenimine. *J. Chem. Soc., Faraday Trans.* 2 **1975**, 71, 1799–1804.
- (44) Fawcett, F. S. Bredt's Rule of Double Bonds in Atomic-Bridged-Ring Structures. *Chem. Rev.* **1950**, *47*, 219–274.